Tailoring Pore Properties of MCM-48 Silica for Selective Adsorption of CO_2

Sangil Kim, Junichi Ida, Vadim V. Guliants,* and Jerry Y. S. Lin†

Department of Chemical and Materials Engineering, University of Cincinnati, Cincinnati, Ohio 45221-0012

Received: September 25, 2004; In Final Form: January 28, 2005

Four different types of amine-attached MCM-48 silicas were prepared and investigated for CO_2 separation from N_2. Monomeric and polymeric hindered and unhindered amines were attached to the pore surface of the MCM-48 silica and characterized with respect to their CO_2 sorption properties. The pore structures and amino group content in these modified silicas were investigated by XRD, FT-IR, TGA, N_2 adsorption/desorption at 77 K and CHN/Si analysis, which confirmed that in all cases the amino groups were attached to the pore surface of MCM-48 at 1.5−5.2 mmol/g. The N_2 adsorption/desorption analysis showed a considerable decrease of the pore volume and surface area for the MCM-48 silica containing a polymeric amine (e.g., polyethyleneimine). The CO_2 adsorption rates and capacities of the amine-attached MCM-48 samples were studied employing a sorption microbalance. The results obtained indicated that in addition to the concentration of surface-attached amino groups, specific interactions between CO_2 and the surface amino groups, and the resultant pore structure after amine group attachment have a significant impact on CO_2 adsorption properties of these promising adsorbent materials.

Introduction

Reducing CO_2 emissions for addressing climate change concerns is becoming increasingly important because the CO_2 concentration in the atmosphere has increased rapidly since industrial revolution. Most currently investigated mitigation processes require CO_2 in a concentrated form. The CO_2 from coal-fired power plants is, however, mixed with N_2, water vapor, oxygen, and other impurities and present at a low ∼15% concentration. Therefore, capturing CO_2 from CO_2 containing streams is an important step for many mitigation methods.

Adsorption and separation of CO_2 over a range of porous solid adsorbents have been widely investigated. The most common physical adsorbents are activated carbons[1] and zeolites, e.g. 4A, 13X, Na-X and Na-A.[1−4] Although these adsorbents possess relatively high CO_2 adsorption capacities, they decline rapidly with increasing temperature. Solid chemical adsorbents, such as hydrotalcite and various basic metal oxides, can reversibly chemisorb CO_2 at high temperatures. For instance, Ding and Alpay reported moderate CO_2 adsorption capacities of 0.65 and 0.58 mmol/g, respectively, on hydrotalcite at 673 and 753 K.[5] Song et al. studied CaO-modified silica and reported the CO_2 adsorption capacity of 0.84 mmol/g at 298 K under 1 atm of CO_2.[6] Sodium oxide-based adsorbents for CO_2 chemisorption were reported by Liang and Harrison, and limestone-derived adsorbents were also reported by Hughes et al.[7,8] Reddy and Smirniotis observed very high CO_2 adsorption capacity of 11.4 mmol/g on Cs-doped CaO.[9] However, all these basic oxide adsorbents suffered from either low CO_2 capacities or severe energy penalties because of high desorption temperatures.

On the other hand, chemical absorption by liquid amines represents the most widely developed commercial technology for CO_2 separation. The most common solvents are alkanolamines, such as monoethanolamine (MEA), diethanolamine (DEA), methyldiethanolamine (MDEA), and triethanolamine (TEA). These amine-based chemical solvents interact specifically with CO_2 and absorb it very selectively.[10−12] However, energy consumption associated with the use of liquid amines is inherently high due to solvent regeneration and large dilutions with water required to prevent equipment corrosion and flow problems caused by viscosity increases with fast-reacting amines. In addition, the overall efficiency of traditional tower stripping design suffers from mass-transfer limitations.[13] However, attachment of amine functional groups to high surface area solids in order to introduce specific interactions with CO_2 represents one possible solution to overcome the limitations of current liquid amine processes for CO_2 separation from dilute sources.

The M41S mesoporous silicas have recently attracted much attention as catalysts, catalyst supports and adsorbents because of their high surface areas, tunable pore sizes and surface chemistry via functionalization. Surface functionalization of mesoporous materials with several types of functional groups for application in adsorption and catalysis has been recently reported.[14−16] However, very few studies appeared on the applications of these materials in gas separation. Moreover, most studies of surface functionalization of mesoporous materials have focused on MCM-41 silica, which has one-dimensional pore channel structure prone to diffusion limitations and pore blockage.[17] Therefore, MCM-48 silica is more attractive than MCM-41 for potential applications in adsorption and heterogeneous catalysis due to its three-dimensional interconnected cubic pore structure.

The introduction of basic sites into the pore channels of mesoporous silica to enhance CO_2 adsorption has been recently investigated by several groups. Shen et al. studied CO_2 adsorption over MCM-41 modified with La_2O_3.[18] Huang et al. reported acid gas removal from natural gas using aminopropyl-attached MCM-48.[19] Chaffee et al. attached various amines to the pores of hexagonal mesoporous silicas (HMS) and characterized them with respect to CO_2 adsorption in a short

* Corresponding author e-mail: vguliant@alpha.che.uc.edu.

† Current address: Department of Chemical and Materials Engineering, Arizona State University, Tempe, AZ 85287-6006.

10.1021/jp045634x CCC: $30.25
Published on Web 03/11/2005

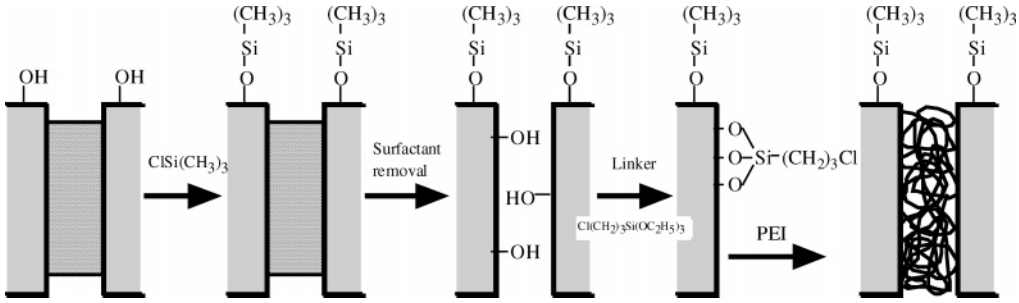

Figure 1. Schematic diagram of PEI attachment to MCM-48 silica.

communication.[20] Hiyoshi et al. also studied grafting of various aminosilanes on mesoporous SBA-15 silica and reported their CO_2 adsorption capacities in a short communication.[21] Chang et al. studied CO_2 adsorption and desorption on aminopropyl-attached SBA-15.[22] Xu et al. modified MCM-41 with polyethylenimine (PEI) and showed 2.6 mmol/g at 348 K and no N_2 adsorption.[23,24] These adsorbent materials display specific interactions with CO_2 and are expected to show high CO_2 selectivity at somewhat elevated temperatures (~373 K) expected for such dilute CO_2 sources as flue gas. However, the attachment of various types of amino groups to the MCM-48 surface and their CO_2/N_2 adsorption properties have not yet been systematically investigated in these brief communications.[18−24] In this study, we investigate the pore structures and CO_2/N_2 adsorption properties of several MCM-48 adsorbents functionalized with four types of amino groups: monomeric unhindered (3-aminopropyl) and hindered (pyrrolidinepropyl), polymerized aminopropyl group and polyethyleneimine (PEI). The fundamental insights obtained in this study are expected to assist in the rational design of novel functionalized M41S adsorbent materials for CO_2 separation from dilute sources.

Experimental Section

Synthesis of MCM-48 Silica. Mesoporous MCM-48 silica was synthesized according to a previously published procedure.[25] In this method, the aqueous micellar solution containing a quaternary ammonium surfactant, $C_{16}H_{33}(CH_3)_3NBr$ (CTAB, Sigma-Aldrich), NaOH, and deionized water was prepared under stirring for 1 h. Then, the solution was added to tetraethyl orthosilicate (TEOS, Alfa-Aesar Chemical). The molar composition of the mixture was 0.59 CTAB:1.0 TEOS:0.5 NaOH: 61 H_2O. The mixture was stirred for 90 min and transferred to an autoclave. The reaction was carried out at 363 K for 96 h. The MCM-48 silica was filtered, washed with deionized water and calcined in air at 723 K for 5 h.

Amine Attachment. MCM-48 powders were reacted with 3-aminopropyltriethoxysilane (3-APTES, Sigma-Aldrich) dissolved in dry toluene under reflux for 2 h to form covalent Si−O−Si bonds with SiOH groups on the mesoporous silica surface. It should be noted that in the absence of water 3-APTES reacts only with surface SiOH groups and 3-APTES polymerization does not occur. Polymerization of 3-APTES inside the MCM-48 pores was also carried out following a similar procedure in the presence of a small amount of water (H_2O/3-APTES = 3:1). In this case, the external surface of as-synthesized MCM-48 prior to CTAB removal was first silylated with trimethylsilane (TMS, Fluka) to avoid the attachment of polymerized 3-APTES to the external surface of MCM-48 because these species were expected to block the entrances to the mesopore channels of MCM-48. CTAB was removed by Soxhlet extraction in a mixture of methanol and HCl at 393 K.

For a hindered amine attachment, such as pyrrolidine, a two-step attachment procedure was employed. The MCM-48 silica was first treated with 3-chloropropyltriethoxysilane followed by the surface N-alkylation with pyrrolidine in toluene. The excess amine was removed by Soxhlet extraction with methylene chloride (CH_2Cl_2) for 8 h at 393 K. Then, the amine-attached MCM-48 silica was dried at room temperature.

For PEI attachment to MCM-48 silica, the chloropropyl-modified MCM-48 silica was functionalized with branched polyethyleneimine (M.W. = 600, Aldrich) by the nucleophilic substitution of the chlorine atom with the amino group in a THF solution for 3 h at 353 K as shown in Figure 1. In this case, the external surface of as-synthesized MCM-48 prior to surfactant removal was first silylated with trimethylsilane to avoid the attachment of PEI to the external surface of MCM-48. Excess PEI was removed by overnight Soxhlet extraction with methanol and HCl at 393 K, and the PEI-modified MCM-48 silica was dried at room temperature. The aminopropyl, pyrrolidinepropyl, polymerized aminopropyl and polyethyleneimine-attached MCM-48 samples are referred to as APS-, PyrPS-, p-APS and PEI-MCM-48, respectively.

Physicochemical Characterization. The powder XRD patterns of MCM-48 silica before and after the amine attachment were recorded on a Siemens D-500 spectrometer using Cu Kα radiation with a step size of 0.02°/s. A BioRad FTS-60 FTIR spectrometer was used to obtain the IR spectra of the amine-attached MCM-48 silica. In situ IR studies were further carried out in order to investigate the mechanism of CO_2 adsorption on the amine-attached MCM-48 silica. For IR measurements, the MCM-48 silica was pressed into a thin wafer and placed in an in situ cell. Prior to CO_2 adsorption, these wafers were outgassed in flowing He (130 mL/min) for 2.5 h at 393 K. The He flow was then replaced with 1.5% CO_2 in He under ambient conditions. After 2 h, the CO_2 atmosphere in the in situ cell was displaced with He and the IR spectra were collected at 4000−1300 cm^{-1}.

The CHN/Si elemental analysis was carried out by Robertson Microlit Laboratories, Inc. (Madison, NJ). The N_2 adsorption−desorption isotherms were collected at 77 K using Micromeritics TriStar 3000 porosimeter. The MCM-48 silica samples were outgassed prior to these measurements at 423 K overnight under N_2 flow. The surface areas were calculated using the BET method, and the pore volumes and pore diameters were calculated by the BJH method.

CO_2 Adsorption on Amine-Attached MCM-48. The CO_2 adsorption properties of the amine-attached MCM-48 samples were studied using a microelectronic recording balance system (CAHN C-1000). The samples were first dried by passing dry He for 3 h at 393 K. After the samples were cooled to the desired temperature (298, 323, 373, and 423 K), CO_2 adsorption was initiated by switching the purge gas from dry He to a CO_2/He

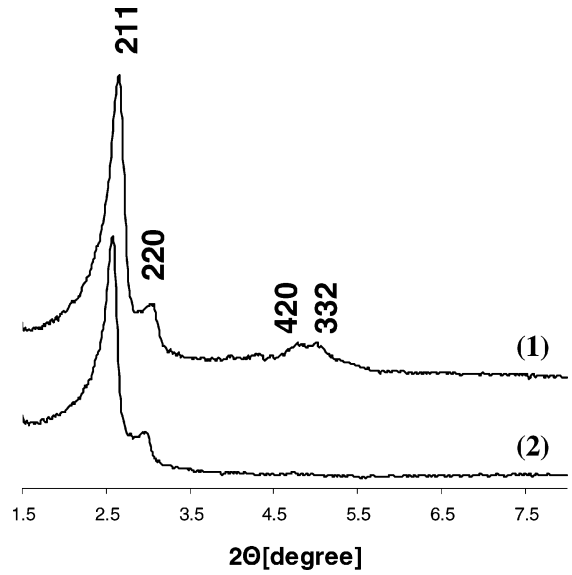

Figure 2. XRD patterns of MCM-48 silica (1) after calcination to remove the surfactant and (2) after 3-aminopropyl group attachment.

gas mixture at different CO_2 concentrations flowing at 150 mL/min. The N_2 adsorption was measured following the same procedure. The CO_2 desorption from the amine-attached MCM-48 silica was investigated after 300−400 min of CO_2 adsorption by ramping the temperature from 298 to 393 K at 0.5 K/min under 1 atm of CO_2.

Results and Discussion

Characterization of Amine Attached MCM-48. The powder X-ray diffraction patterns (XRD) of the MCM-48 silica before and after the 3-aminopropyl group attachment are shown in Figure 2. The XRD patterns displayed Bragg peaks in the $2\theta = 1.5-8°$ range, which can be indexed to different *hkl* reflections. These *d*-spacings were indicative of MCM-48 structure possessing the cubic *Ia*3*d* space group.[26] The XRD patterns of the as-synthesized and calcined mesoporous MCM-48 powders consisted of the typical reflection at 2.5° (211) and weak reflections at 2.9° (220), 4.7° (420), and 4.9° (332) which corresponded to the *d*-spacings of ca. 34.8, 30.3, 18.8, and 19.0 Å, respectively. The XRD patterns of MCM-48 did not change significantly after amino group attachment. The peak intensity, however, decreased slightly, and the peaks with higher *hkl* indices, i.e., (420) and (332), almost completely disappeared. The (211) peak shifted to a slightly lower 2θ angle ($2\theta = 2.51°$ and $d_{211} = 35.1$ Å) after the introduction of aminopropyl groups, as compared to the calcined MCM-48 ($2\theta = 2.54°$ and $d_{211} = 34.8$ Å). In the case of M41S materials, the peak intensity is a function of the scattering contrast between the silica walls and pore channels and, in general, decreases with decreasing scattering contrast after attachment of organic groups to the pore surface.[27] Therefore, the observed decrease of the XRD peak intensity is probably due to the pore filling by aminopropyl groups. Disappearance of higher *hkl* peaks may be due to the lower structural order of aminopropyl attached MCM-48. Previous studies of functionalization of mesoporous silica have reported similar changes.[14,23]

The IR spectra of original and amine-attached MCM-48 samples are shown in Figure 3. A sharp absorption band at 3748 cm^{-1} and a broad absorption band at around 3500 cm^{-1} present in the IR spectra of the original MCM-48 are assigned to single SiOH and hydrogen-bonded SiOH groups, respectively.[28] The band of single SiOH groups almost completely disappeared after

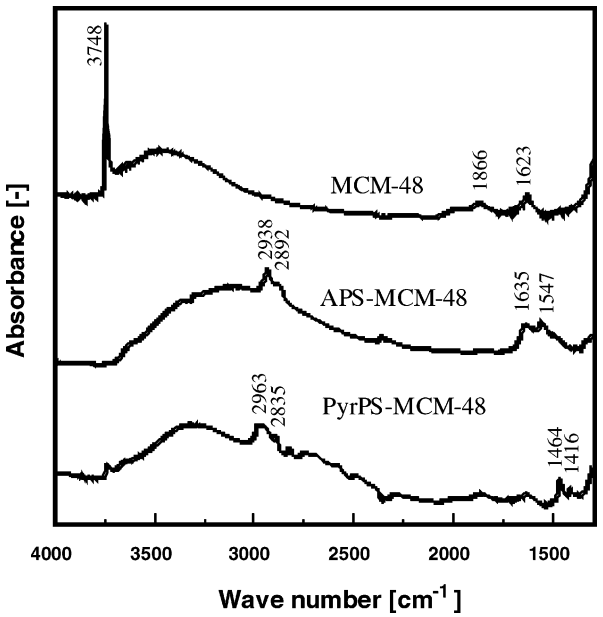

Figure 3. IR spectra of the original and amine-attached MCM-48.

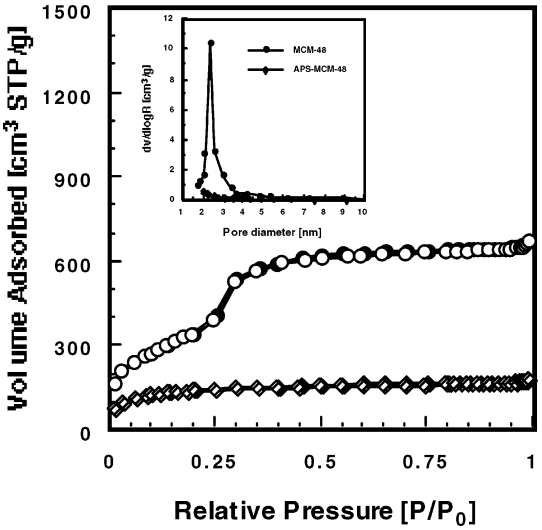

Figure 4. The N_2 adsorption−desorption isotherms of MCM-48 powders at 77 K (1) before and (2) after aminopropyl (APS) group attachment.

amine group attachment (for both APS- and PyrPS-MCM-48). This indicated that almost all single SiOH groups were consumed during the attachment of functional groups. The broad absorption band, however, can still be observed at 3100−3300 cm^{-1} shifted from 3500 cm^{-1} after amine group attachment (for both APS- and PyrPS-MCM-48). This suggested that hydrogen-bonded SiOH remained after the amine group attachment. Zhao et al. reported that only the free and geminal SiOH groups (i.e., single SiOH groups) are able to react with various silanes, while hydrogen-bonded ones were unreactive.[29] Furthermore, some SiOH groups may be inaccessible for the surface functionalization with silanes. Our results are in agreement with these previous observations. The IR bands at 2963−2938 and 2892−2835 cm^{-1} are due to the CH_2 stretching modes of the propyl chain. The absorption band at 1635 cm^{-1} can also be assigned to the NH_2 scissor in the case of APS-MCM-48.[14] The bands at 1464 and 1416 cm^{-1} are assigned to a C−H stretch in a cyclic amine in the case of PyrPS-MCM-48.[10]

The N_2 adsorption−desorption isotherms at 77 K for the original and APS-MCM-48 samples are shown in Figure 4. The

TABLE 1: Structural Properties of Original and Amine-Attached MCM-48 Silicas[a]

sample	BET surface area [m^2/g]	BJH ads. pore volume [cm^3/g]	BJH ads. pore diameter [nm]	wt % N	AGC [mmol/g]
MCM-48	1290	1.15	2.58		
APS-MCM-48	505	0.13	MP	3.42	2.45
PyrPS-MCM-48	507	0.45	MP	2.07	1.48
p-APS-MCM-48	5.0	0.01	NP	5.58	3.99
PEI-MCM-48	58.4	0.02	NP	7.28	5.20

[a] AGC = amine group content. MP = microporous. NP = nonporous.

N_2 adsorption isotherm of the original MCM-48 is a typical reversible type IV adsorption isotherm characteristic of mesoporous material, while that of the APS-attached MCM-48 is type I microporous. The mesoporous character of the original MCM-48 silica reflected in an S-shaped adsorption isotherm was lost after the aminopropyl group attachment. The APS-MCM-48 showed the presence of microporosity, which demonstrates the effect of the aminopropyl group attachment on the pore structure of the MCM-48 silica. A significant decrease in the surface areas and pore volumes were also observed upon amine attachment. The specific BET surface area, pore volumes and pore sizes of the original and amine-attached MCM-48 samples are summarized in Table 1. As compared to monomeric amine-attached silica, i.e., APS- and PyrPS-MCM-48, polymeric amine containing MCM-48, p-APS- and PEI-MCM-48 silicas showed a more significant decrease of the surface areas and pore volumes, probably due to significant pore filling with functional groups. In particular, p-APS-MCM-48 lost nearly all surface area and pore volume after reaction with polymerized 3-APTES, which indicated nearly complete pore filling.

The surface coverage of 3-aminopropyl- and pyrrolidinepropyl groups was calculated on the basis of the nitrogen content obtained from the CHN/Si elemental analysis. It indicated that 2.5 mmol/g (1.1 molecule/nm^2) of 3-aminopropyl groups and 1.5 mmol/g (0.7 molecule/nm^2) of pyrrolidinepropyl groups were attached to the MCM-48 pore surface. The attached amine content found in this study is similar to that for aminopropyl groups attached to MCM-41 (1.5 mmol/g) reported by Yoshitake et al.[14] and also to that for aminopropyl groups attached to MCM-48 (2.3 mmol/g) reported by Huang and Yang.[19] Both original mesoporous silicas employed in these studies had similar pore size and surface area (2.9 nm and 1283 m^2/g for MCM-41[14] and 1389 m^2/g for MCM-48[19]) to the MCM-48 silica of our study. Lower loading of amino groups in PyrPS-MCM-48 is possibly due to the larger size of pyrrolidinepropyl as compared to aminopropyl groups.[14,28] Such loadings of surface amino groups may be rationalized in terms of the concentration of reactive SiOH groups on the pore surface of MCM-48. Zhao et al. reported that MCM-41 contained 2.5-3.0 SiOH/nm^2.[29] However, their results indicated that only 0.7−1.9 SiOH/nm^2 depending on outgassing conditions were reactive toward silane coupling agents and that H-bonded SiOH groups were unreactive. Our IR data further confirmed that the free SiOH groups disappeared and H-bonded silanols remained after the amine attachment. Kumar et al.[30] reported that the concentration of the surface SiOH groups was about 1.8 SiOH/nm^2 on the MCM-48 surface. Since this value includes both reactive single SiOH groups and also unreactive hydrogen-bonded SiOH groups, the surface concentrations of aminopropyl groups and pyrrolidinepropyl groups obtained in this study are consistent with these previous observations.

PEI-MCM-48 and p-APS-MCM-48 silicas showed higher N content as compared to the samples containing monomeric amines (APS and PyrPS-MCM-48). This was expected since polyethyleneimine and polymeric aminopropyl siloxane species can fill the entire pore volume, while discrete aminopropyl and pyrrolidinepropyl groups were attached to the pore surface only.

Thermogravimetric (TGA) weight loss curves for the original and amine-attached MCM-48 samples are shown in Figure 5. All samples showed weight loss below 373 K associated with physically adsorbed water. Above 373 K, the TGA curve for the original MCM-48 sample showed additional weight loss associated with condensation of surface silanol groups. The amine-attached MCM-48 samples showed minor weight loss up to 450 K. Above this temperature, they exhibited a weight loss behavior very different from that of the original MCM-48 sample. The weight loss above 473 K was associated with the decomposition of the surface-attached amines as well as the condensation of SiOH groups.[28] When compared to monomeric amine-attached samples, MCM-48 containing polymeric amines showed a greater weight loss due to the higher content of polymeric amines inside the MCM-48 mesopores. These results are in agreement with the pore characterization and elemental analysis data of the amine attached MCM-48 materials.

CO_2 Adsorption and CO_2/N_2 Equilibrium Selectivities. The CO_2 uptake of the amine-attached MCM-48 samples in pure CO_2 atmosphere ($P_{CO_2} = 1$ atm) at 298 K is shown in Figure 6. The CO_2 adsorption capacities of the amine-attached MCM-48 samples after 40 min of CO_2 adsorption were 0.8, 0.4, 0.3, and 0.1 mmol/g for APS, PEI, PyrPS, and p-APS-MCM-48, respectively. APS-MCM-48 displayed the highest CO_2 adsorption rate and capacity under these experimental conditions despite the relatively low concentration of surface amino groups. This indicated that in addition to the concentration of surface amino groups, other factors, e.g., the strength of CO_2-amine interactions and accessibility of amino groups, were important for CO_2 adsorption rate and capacity. Since the pyrrolidinepropyl group has a hindered structure of a tertiary amine, PyrPS-MCM-48 interacted with CO_2 more weakly as compared to APS-MCM-48 resulting in lower CO_2 uptake rate and capacity. This will be discussed in more detail below.

Despite high surface concentration of amino groups in the case of p-APS- and PEI-MCM-48, these samples displayed slower CO_2 uptake rate and lower CO_2 adsorption capacities, in particular in the case of p-APS-MCMC-48. It should be noted here that both APS- and p-APS-MCM-48 samples were prepared using 3-aminopropyltriethoxysilane. In the latter case, APS was allowed to undergo partial hydrolysis and oligomerization before attachment of oligomerized aminopropyl siloxane species to the MCM-48 mesopores. Therefore, the slower CO_2 uptake rates and lower CO_2 adsorption capacities in the case of p-APS and PEI-MCM-48 may be explained by significant changes in the pore structure after the amine group attachment. According to the surface area and pore size data, the pores of p-APS-MCM-48 were almost completely filled with attached polymerized aminopropyl groups. This resulted in significant mass-transfer limitations manifested in a very low CO_2 uptake rate. Although, the pores of PEI-MCM-48 were not blocked completely, the pore volume and surface area were low (58.4 m^2/g and 0.02 cm^3/g, respectively). PEI-MCM-48 also suffered from the mass-transfer limitations, despite the fact that it had the highest concentration of the amine adsorption sites. Xu et al. also reported that CO_2 adsorption on PEI-attached MCM-41 at low temperature was a diffusion-controlled process.[23] They reported a higher CO_2 adsorption capacity at 348 K than 323 K on PEI-

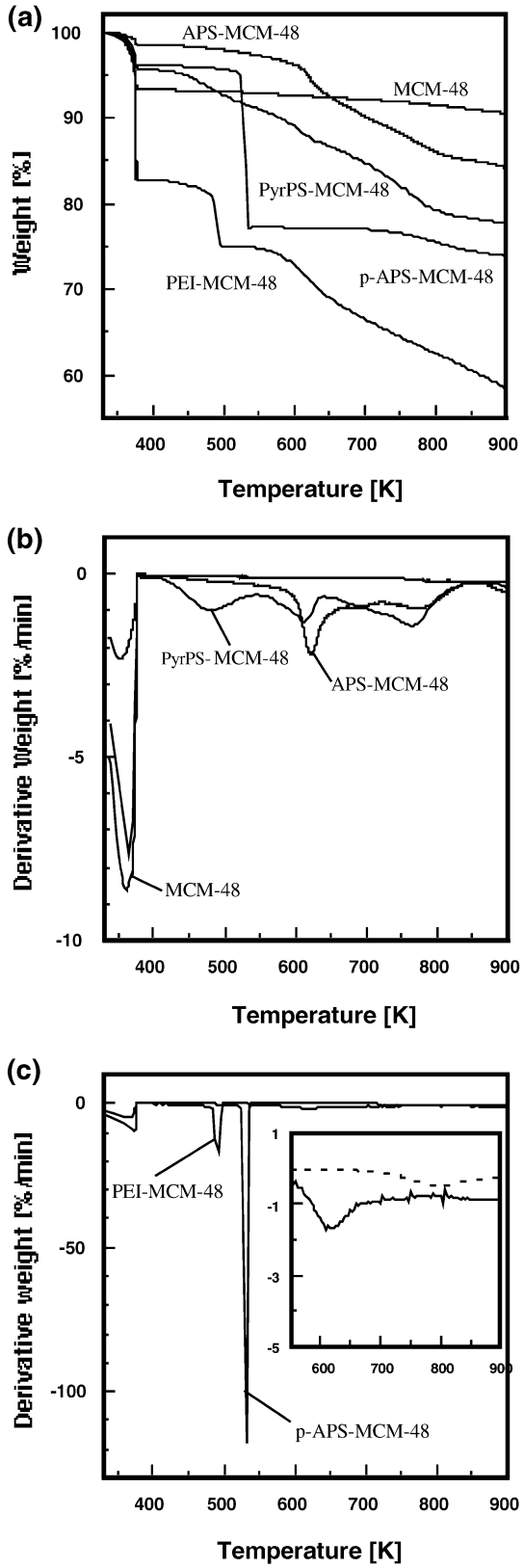

Figure 5. TGA weight loss curves of MCM-48 silicas in air. (a) TGA curves for the original and amine attached MCM-48, (b) DTG curves for the monomeric amine attached MCM-48, and (c) DTG curves for the polymeric amine attached MCM-48.

attached MCM-41 because of the increased CO_2 accessibility to CO_2 adsorption sites at higher temperature.

We further examined the effect of temperature on CO_2 adsorption on PEI-MCM-48 shown in Figure 7. As the temperature was increased from 323 to 373 K, the CO_2 uptake rate also increased. Although this behavior is opposite from what was expected based on thermodynamic considerations of CO_2 adsorption on PEI, it may be explained by the increase of CO_2 diffusion rate at higher temperature. Although the total equilibrium CO_2 adsorption capacity decreased with temperature, the number of CO_2 adsorption sites accessible to CO_2 increased because of the increase in CO_2 diffusivity at high temperature. Decrease of CO_2 uptake at 423 K is probably due to the PEI decomposition, which is further supported by the TGA data.

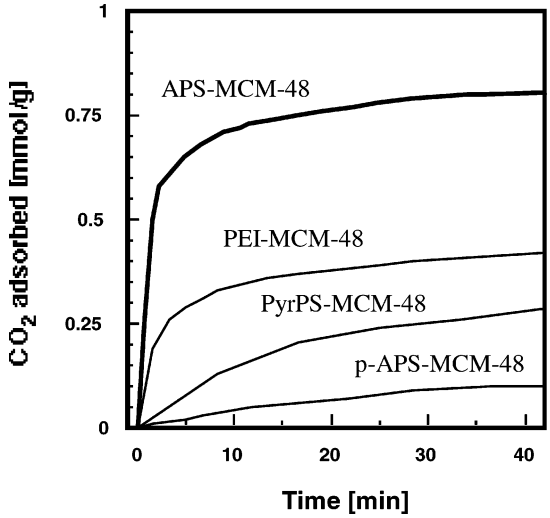

Figure 6. CO_2 uptake on amine-attached MCM-48 at 298 K (P_{CO_2} = 1 atm).

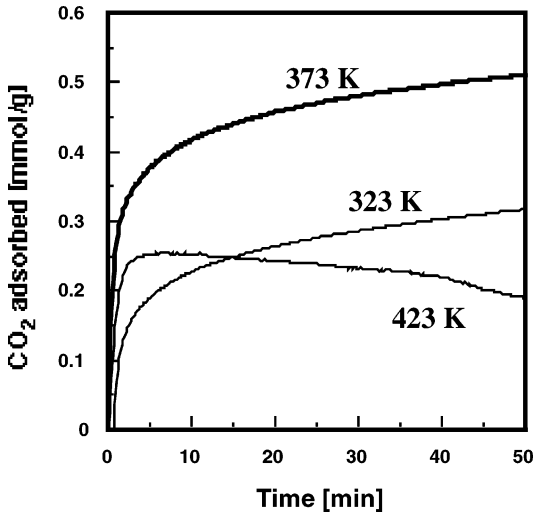

Figure 7. CO_2 uptake on PEI-MCM-48 (P_{CO_2} = 1 atm).

The CO_2 desorption from the amine-attached MCM-48 silicas at 298−393 K under 1 atm of CO_2 is shown in Figure 8. The CO_2 desorption from APS- and PyrPS-MCM-48 are shown in Figure 8a and b. These results demonstrated that as expected CO_2 increasingly desorbed in both cases as the temperature increased. The CO_2 desorption from APS-MCM-48 was slower than from PyrPS-MCM-48. This indicated that the interactions between the pyrrolidinepropyl groups and CO_2 are weaker than those between the aminopropyl groups and CO_2 which is in agreement with the results of CO_2 adsorption experiments. In both cases, CO_2 desorption was observed at low temperature (<50 °C) even under 1 atm of CO_2.

The CO_2 desorption data from p-APS- and PEI-MCM-48 at 298−393 K under 1 atm of CO_2 are shown in Figure 8c and d. These two polymerized amine-attached MCM-48 silicas showed

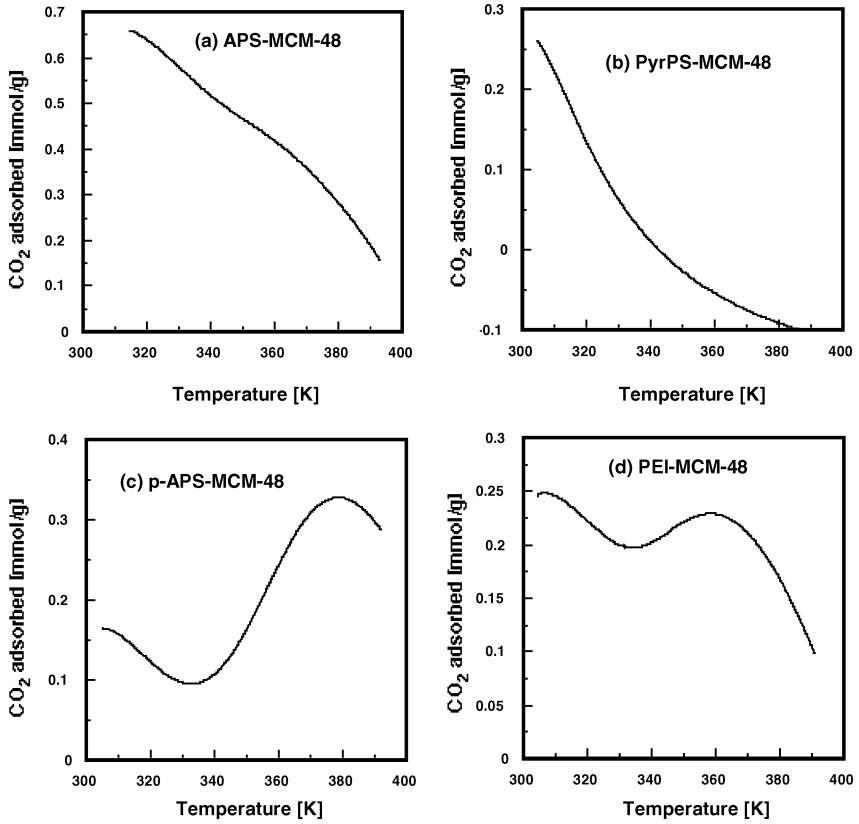

Figure 8. CO_2 desorption from the amine-attached MCM-48 silicas ($P_{CO_2} = 1$ atm).

interesting CO_2 desorption behavior. It can be seen that the CO_2 desorption occurred initially as the temperature increased. However, above 335 K CO_2 adsorption seemingly occurred, and the adsorbed amount even exceeded the amount adsorbed at 298 K. A further temperature increase resulted in CO_2 desorption. Although the CO_2 desorption experiments were conducted after 300−400 min of CO_2 adsorption at room temperature, the adsorption equilibrium was not achieved in the cases of p-APS and PEI-MCM-48 because significant pore filling in these materials resulted in a slow CO_2 adsorption rate. Therefore, although p-APS and PEI-MCM-48 contained a high concentration of CO_2 adsorption sites, only a fraction of these sites were accessible to CO_2 after 300−400 min of exposure at 298 K. The temperature increase is expected to affect CO_2 adsorption in two mutually opposing ways by (i) increasing CO_2 diffusivity and enhancing the accessibility of vacant adsorption sites and (ii) decreasing equilibrium CO_2 adsorption capacity. As expected, the CO_2 adsorption capacity decreases initially as the temperature is increased. However, as the temperature is increased further, enhanced CO_2 diffusivity and accessibility of vacant adsorption sites results in an apparent increase of CO_2 adsorption capacity. Above 375 K for p-APS-MCM-48 and 360 K for PEI-MCM-48, the temperature effect on the equilibrium CO_2 adsorption capacity becomes a dominant trend again resulting in the observed resumption of CO_2 desorption.

To examine the effect of steric hindrance on CO_2 adsorption, the CO_2 adsorption isotherms on the APS and PyrPS-MCM-48 at 293 K were measured (Figure 9). In Figure 9, CO_2 adsorption capacities are expressed as CO_2 adsorbed per surface amine site. The CO_2 adsorption capacity of APS-MCM-48 rapidly increased with P_{CO_2} at $P_{CO_2} < 0.2$ atm. At $P_{CO_2} = 0.2$ atm, the adsorption capacity was 0.25 mmol/mmol-amine. At higher P_{CO_2}, the adsorption capacity increased slightly with P_{CO_2} and reached 0.35 mmol/mmol-amine at $P_{CO_2} = 1.0$ atm. On the other hand, the CO_2 adsorption on the PyrPS-MCM-48 was characterized

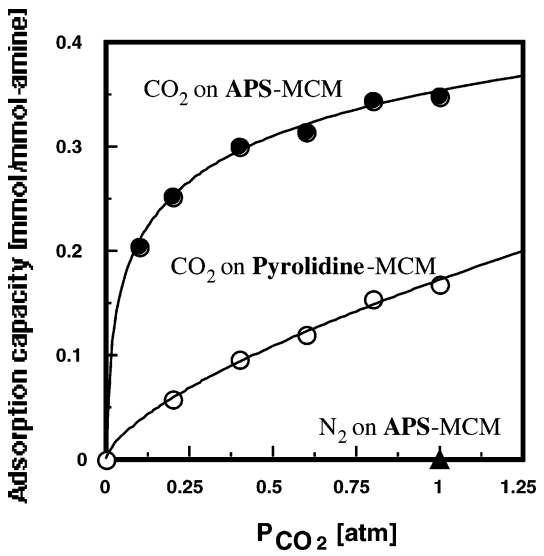

Figure 9. CO_2 and N_2 adsorption on APS- and PyrPS-MCM-48 at 298 K.

by lower CO_2/surface amine ratios (0.17) suggesting that the hindered amine geometry of the surface pyrrolidine groups resulted in weaker CO_2-amine interactions. In the absence of water, it is believed that CO_2 adsorption at primary amine sites proceeds via formation of surface carbamate groups, e.g. for the aminopropyl attached MCM-48 (APS-MCM-48):

$$2R{-}NH_2 + CO_2 \rightarrow RNHCOO^- + RNH_3^+ \qquad (1)$$

This indicates that two amino groups chemisorb one CO_2 molecule (CO_2/surface amine ratios = 0.5). The CO_2/surface amine ratios observed in our study is indeed close to this theoretical value. Moreover, in situ IR spectra also supported

the surface carbamate formation (not shown here). However, in the case of tertiary amines, i.e., pyrrolidine, the carbamate formation did not occur.[31] In situ IR spectra indicated the absence of carbamate species during CO_2 adsorption on PyrPS-MCM-48 (not shown here). Therefore, weak interactions between CO_2 and tertiary amines led to low CO_2/amine ratios observed for PyrPS-MCM-48.

The N_2 adsorption experiments were also performed following the same procedure at 298 K. The results obtained shown for a representative APS-MCM-48 indicated that N_2 adsorption on functionalized MCM-48 silicas of this study was negligible (Figure 9). Therefore, although the CO_2 adsorption capacity of APS-MCM-48 is lower than that of a commercial CO_2 adsorbent, e.g. zeolite 13X at 1 atm and at 298 K (4.7 mmol/g),[32] APS-MCM-48 displayed much higher CO_2/N_2 selectivity ($\gg$100 vs $\sim$16 for zeolite X).

Conclusions

The effect of several types of amino groups present in the pores of MCM-48 on its CO_2 adsorption properties was examined employing monomeric and polymeric hindered and unhindered amines, such as aminopropyl (monomeric, unhindered), pyrrolidinepropyl (monomeric, hindered), polymerized aminopropyl (polymeric, unhindered) groups and PEI (polymeric, hindered). Although the MCM-48 silica containing polymeric amines showed a high concentration of amine sites, the monomeric aminopropyl-attached MCM-48 displayed the highest CO_2 adsorption rate at 298 K because of greater accessibility of amine adsorption sites. APS-MCM-48 also displayed high equilibrium selectivity in adsorptive CO_2/N_2 separation indicating the promise of these molecularly engineered materials for adsorptive separation of CO_2. The results obtained indicated that in addition to the concentration of surface-attached amino groups, specific interactions between CO_2 and the surface amino groups and the resultant pore structure after amine group attachment have a significant impact on CO_2 adsorption properties of these promising adsorbent materials.

Acknowledgment. This research was supported by Ohio Coal Development Office (OCDO, Subcontract OCRC3-00-1.C3.14).

References and Notes

(1) Siriwardane, R. V.; Shen, M. S.; Fisher, E. P.; Poston, J. A. *Energy Fuels* **2001**, *15*, 279.

(2) Na, B, K.; Lee, H.; Koo, K. K.; Song, H. K. *Ind. Eng. Chem. Res.* **2002**, *41*, 5498.

(3) Gomes, V. G.; Yee, K. W. K. *Sep. Purif. Technol.* **2002**, *28*, 161.

(4) Takamura, Y.; Narita, S.; Aoki, J.; Hironaka, S.; Uchida, S. *Sep. Purif. Technol.* **2001**.

(5) Ding, Y.; Alpay, E. *Chem. Eng. Sci.* **2000**, *55*, 3461.

(6) Song, H. K.; Cho, K. W.; Lee, K. H. *J. Non-Crystalline Solids* **1998**, *242*, 69.

(7) Liang, Y.; Harrison, D. P. *Energy Fuels* **2004**, *18*, 569.

(8) Hughes, R. W.; Lu, D.; Anthony, E. J.; Wu, Y. *Ind. Eng. Chem. Res.* **2004**, *43*, 5529.

(9) Reddy, E. P.; Smirniotis, P. G. *J. Phys. Chem. B* **2004**, *108*, 7794.

(10) Mimura, T.; Simayoshi, H.; Suda, T.; Iijima, M.; Mituoka, S. *Energy Conserv. Management, Suppl.* **1997**, *38*, S57.

(11) Leci, C. L. *Energy Conserv. Management, Suppl.* **1997**, *38*, S57.

(12) Critchfield, J. E.; Su, W. Y.; Kenney, T. J.; Holub, P. E. US Patent 5,861,051, 1996.

(13) Martin, J. E.; Anderson, M. T.; Odink, J.; Newcomer, P. *Langmuir* **1997**, *13*, 4133.

(14) Yoshitake, H.; Yokoi, T.; Tatsumi, T. *Chem. Mater.* **2002**, *14*, 4603.

(15) Fryxell, G. E.; Liu, J.; Hauser, T. A.; Nie, Z.; Ferris, K. F.; Mattigod, S.; Gong, M.; Hallen, R. T. *Chem. Mater.* **1999**, *11*, 2148.

(16) Lin, X.; Chuah, G. K.; Jaenicke, S. *J. Mol. Catal. A: Chem.* **1999**, *150*, 287.

(17) Kruk, M.; Jaroniec, M.; Pena, M. L.; Rey, F. *Chem. Mater.* **2002**, *14*, 4434.

(18) Shen, S. C.; Chen, X.; Kawi, S. *Langmuir* **2004**, *20*, 9130.

(19) Huang, H. Y.; Yang, R. T.; Chinn, D.; Munson, C. L. *Ind. Eng. Chem. Res.* **2003**, *42*, 2427.

(20) Chaffee, A. L.; Delaney, S. W.; Knowles, G. P. *Abstr. Pap. Am. Chem. Soc.* **2002**, 223.

(21) Hiyoshi, N.; Yogo, K.; Yashima, T. *Chem. Lett.* **2004**, *33*, 510.

(22) Chang, A. C. C.; Chuang, S. S. C.; Gray, M.; Soong, Y. *Energy Fuels* **2003**, *17*, 468.

(23) Xu, X.; Song, C.; Anderson, J. M.; Miller, G. B.; Scaroni, A. W. *Energy Fuels* **2002**, *16*, 1463.

(24) Xu, X.; Song, C.; Andresen, J. M.; Miller, B. G.; Scaroni, A. W. *Microporous Mesoporous Mater.* **2003**, *62*, 29.

(25) Nishiyama, N.; Park, D.; Koide, A.; Egashira, Y.; Ueyama, K. *J. Mem. Sci.* **2001**, *182*, 235.

(26) Tomski, P. 1st Ohio Carbon Dioxide Reduction, Sequestration and Capture Forum, 2001.

(27) Mercier, L.; Pinnavaia, T. J. *Environ. Sci. Technol.* **1998**, *32*, 2749.

(28) Jaroniec, C. P.; Kruk, M.; Jaroniec, M.; Sayari, A. *J. Phys. Chem. B* **1998**, *102*, 5503.

(29) Zhao, X. S.; Lu, G. Q.; Whittaker, A. K.; Millar, G. J.; Zhu, H. Y. *J. Phys. Chem. B* **1997**, *101*, 6525.

(30) Kumar, D.; Schumacher, K.; Hohenesche, C. du F. von; Grun, M.; Unger, K. K. *Colloids Surf., A* **2001**, *187*−*188*, 109.

(31) Suda, T.; Iijima, M.; Tanaka, H.; Mitsuoka, S.; Iwaki, T. *Environ. Prog.* **1997**, *16*, 200.

(32) Cavenati, S.; Grande, C. A.; Rodrigues, A. E. *J. Chem. Eng. Data* **2004**, *49*, 1095.